This is a repository copy of *On the onset of dust formation in AGB stars*.

White Rose Research Online URL for this paper:
http://eprints.whiterose.ac.uk/156852/

Version: Accepted Version

On the onset of
dust formation in AGB stars

David Gobrecht[1], Stefan T. Bromley[2],[3], John M. C. Plane[4], Leen Decin[1] and Sergio Cristallo[5],[6]

[1]Institute of Astronomy, KU Leuven, B-3001, Leuven, Belgium
email: david.gobrecht@kuleuven.be

[2]Departament de Ciència de Materials i Química Física & Institut de Química Téorica i Computacional (IQTCUB), Universitat de Barcelona, E-08028 Barcelona, Spain

[3]Institució Catalana de Recerca i Estudis Avançats (ICREA), E-08010 Barcelona, Spain

[4]School of Chemistry, Leeds University, Box 515, GB-75120 Leeds, Great Britain

[5]INAF - Osservatorio Astronomico dAbruzzo, Via mentore maggini, I-64100 Teramo, Italy

[6]INFN - Sezione di Perugia, via A. Pascoli, I-06123, Perugia, Italy

Abstract. A promising candidate to initiate dust formation in oxygen-rich AGB stars is alumina (Al_2O_3) showing an emission feature around $\sim 13\mu$m attributed to $Al-O$ stretching and bending modes (Posch *et al.* (1999), Sloan *et al.* (2003)). The counterpart to alumina in carbon-rich AGB atmospheres is the highly refractory silicon carbide (SiC) showing a characteristic feature around 11.3μm (Treffers & Cohen (1974)). Alumina and SiC grains are thought to represent the first condensates to emerge in AGB stellar atmospheres. We follow a bottom-up approach, starting with the smallest stoichiometric clusters (i.e. Al_4O_6, Si_2C_2), successively building up larger-sized clusters. We present new results of the quantum-mechanical structure calculations of $(Al_2O_3)_n$, $n =1-10$ and $(SiC)_n$ clusters with $n =1-16$, including potential energies, rotational constants, and structure-specific vibrational spectra. We demonstrate the energetic viability of homogeneous nucleation scenarios where monomers (Al_2O_3 and SiC) or dimers (Al_4O_6 and Si_2C_2) are successively added. We find significant differences between our quantum theory based results and nanoparticle properties derived from (classical) nucleation theory.

Keywords. dust formation, molecular clusters, nucleation, alumina, silicon carbide, global optimisation, bottom-up, chemical-kinetics

1. Introduction

Cosmic dust is crucial for the evolution of galaxies. It impacts the synthesis of complex organic molecules in molecular clouds, the wind-driving of evolved stars and the formation of celestial bodies (e.g. asteroids, planets) in protoplanetary discs (Henning (2010)). Asymptotic Giant Branch (AGB) stars represent a major contributor to the global dust budget in galaxies. The chemistry in the inner circumstellar envelopes of AGB stars (i.e. dust formation zone, $R =1-10$ R$_*$) is primarily controlled by the carbon-to-oxygen (C/O) ratio. The CO molecule is triple bonded and very stable (dissociation energy of 11.1 eV) (see e.g. Habing & Olofsson (2004)). As a consequence the lesser abundant element (C or O) is predominantly locked up in the CO molecule leaving little room to form other molecules than CO. Many molecular abundances can be approximated to a great extent with thermodynamic equilibrium calculations.
However, this simple picture is challenged as carbon-bearing molecules (HCN, CS, CO_2) have been observed in O-rich AGB stars (Lindqvist *et al.* (1988), Decin *et al.* (2010)A, Justtanont *et al.* (1998)) and oxygen-bearing species (H_2O, SiO) were found in C-rich

AGB atmospheres (Decin *et al.* (2010)B, Neufeld *et al.* (2011), Johansson *et al.* (1984)). Their presence can only be explained by processes deviating from chemical and thermal equilibrium. CO might be dissociated by shock-induced collisions (Gobrecht *et al.* (2016)), or by interstellar photons (Agúndez *et al.* (2010), Van de Sande *et al.* (2018)) where free C and O are released to form other unexpected molecular species. In contrast to the above mentioned molecules, the dust condensates are carbonaceous in C/O>1 environments and oxygen-rich in oxygen-dominated (C/O<1) regimes.

In the latter case, metal oxides represent the majority of the solids as there are no stable, pure oxygen compounds larger than ozone (O_3). The main dust component in oxygen-rich AGB stars are silicates. Silicates are composed of a least three elements (Si, O and Mg) and are so called ternary oxides. Iron (Fe) might be incorporated in the Mg-rich silicate grains at a later stage and act as a thermostat for the grain (Woitke (2006)). In this case, the dust grains are quaternary oxides consisting of O, Si, Mg and Fe. Measurements on the vapor pressure of Mg-rich silicate grains as well as on pure silicon oxide (SiO) resulted in rather low condensation temperatures ($800-1000$ K) for pressures that prevail in the circumstellar envelopes (Wetzel *et al.* (2013)). Recent ALMA observations have shown that the silicate features around 10 μm and 18μm are absent for the low mass-loss rate stars W Hydrae and R Doradus (Decin *et al.* (2017)), but they are present in the high mass loss rate object IK Tau. Theses findings indicate that, albeit silicates represent the main component of oxygen-rich dust grains, they are not the first condensates to emerge in the outflows of M-type AGB stars. The first condensate, or *seed* particle, initiating the nucleation process is supposed to have a high condensation temperature, made up from available and abundant elements and molecules, and sufficiently fast growing rates in circumstellar conditions. There are several metal oxides satisfying the above conditions: Titania (TiO_2), Magnesia (MgO), silicon monoxide (SiO) and alumina (Al_2O_3). In crystalline form, titania, or TiO_2, exist as anatase and rutile that are both highly refractory. However, the solar titanium abundance is rather low. Silicon monoxide (SiO) is fairly abundant in the envelopes of AGB stars, though its nucleation is rather unlikely to occur in circumstellar media (Bromley *et al.* (2016)). On one hand, a homogeneous nucleation is hampered by energetic barriers (Goumans & Bromley (2012)). On the other hand, Si starts to segregate and to form islands inside the most stable clusters for small cluster sizes $(SiO)_n$, $n \geqslant 10$. The nucleation of MgO clusters was investigated by Köhler *et al.* (1997). They found that the nucleation rate of MgO turns out to be too small to form the seed nuclei for silicate dust formation. One reason are the "magic" cluster sizes (2, 4, 6, 9, 12 and 15 MgO units) with enhanced stability that hamper the formation of larger sized clusters. A promising candidate to initiate dust formation in oxygen-rich AGB stars is alumina (stoichiometric formula Al_2O_3) as its nucleation is not constrained by atomic segregation or energy barriers as we will show below. Circumstellar alumina shows a spectral emission feature around $\sim$13 μm attributed to Al$-$O stretching and bending modes (Posch *et al.* (1999), Sloan *et al.* (2003)). This feature has been seen in several oxygen-rich AGB sources (S Ori, R Cnc, GX Mon, W Hya, R Dor) close to the stellar surface at around $2-3$ R$_*$ (Karovicova *et al.* (2013), Decin *et al.* (2017)). In the case of carbon AGB stars, it is argued that the nucleation of pure or hydrogenated (amorphous) carbon is sufficient to explain the observed mass loss rates (Höfner *et al.* (2003)). However, silicon carbide (SiC) may also play an important role in the nucleation of carbon dust owing to its high thermal stability and its presence in meteorites.
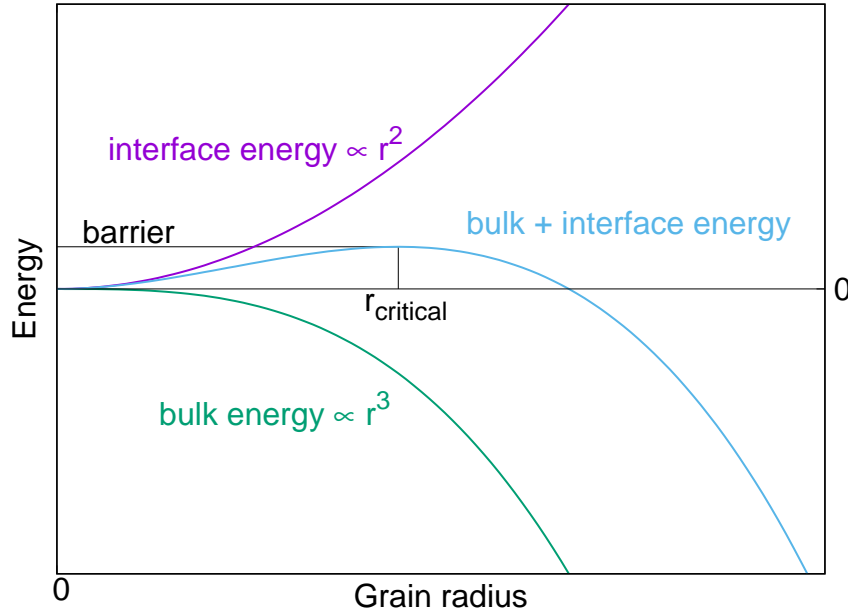
Figure 1. Schematic sketch of the classical nucleation energy versus particle radius (size) in blue. The bulk component is in green, and the interface component is in violet .

2. Global optimisation methods

Top-down chemical methods use a known macroscopic ensemble of atoms (e.g. a crystal structure) and interpolate the unknown properties and characteristics of smaller-sized systems like nanoparticles and molecular clusters. A prime example of a physio-chemical top-down approach is Classical Nucleation Theory (CNT). In CNT, many generic properties of a particle with size N can be expressed as a sum of a bulk term and a surface interface) term. This is also true for the potential and free energies of the particles, i.e. $E_{pot} = E_{surface} + E_{bulk}$. An illustrative example is shown in Figure 1.

The surface (interface) energy can be interpreted as a sort of surface tension. It is repulsive and scales with the particle size (or radius) as r^2. The volume (bulk) term is attractive and scales with the grain radius as r^3. The resulting curve considering both, bulk and interface, has a maximum for r>0. The maximum is located at the so called critical radius r_{crit} and has a value E_{crit} corresponding to an energy barrier. In the CNT regime, E_{crit} represent the energetic bottleneck of the nucleation process. Once this barrier is overcome (i.e. the dust particle has grown to a radius of r_{crit}), the subsequent nucleation is energetically favourable. However, it has been shown that the global minima structures of a variety of (sub-)nanosized clusters, including TiO_2 (Lamiel-Garcia *et al.* (2017)), SiO (Bromley *et al.* (2016)), MgO (Chen *et al.* (2014)), and Al_2O_3 (Li & Cheng (2012)), as well as SiC (Gobrecht *et al.* (2017)) do not exhibit bulk-like geometries. In contrast, potential and free energies, bond lengths and angles, atomic coordination, and formal charges deviate significantly from bulk-like analogues (bulk cuts). We conclude that classical nucleation theory cannot be made to work for small clusters representing the basic building blocks of (circumstellar) dust. We use a bottom-up approach starting with molecules and molecular clusters, and successively build up larger sized dust clusters and dust grains. We are convinced that the formation

Table 1. The parameter ranges used in this study to compute the inter-atomic Buckingham pair potential. Charges q and q are given in atomic units, A in eV, B in Å C in eV Å^{-6}.

q(Al)	q(O)	A(Al-O)	B(Al-O)	C(Al-O)	A(O-O)	B(O-O)	C(O-O)
+3	-2	2409.5	0.2649	0.0	25.410	0.6937	32.32

q(Si)	q(C)	A(Si-C)	B(Si-C)	C(Si-C)	A(C-C)	B(C-C)	C(C-C)
+2	-2	592.34	0.3521	12.897	25.410	0.6937	32.32

of condensates are described more realistically using a bottom-up approach, as it mimics the onset of dust formation in expanding circumstellar shells. In order to reduce the enormous computational cost arising in quantum-chemical bottom-up approaches, we generate a number (typically ∼100 for each size) of candidate cluster structures among of millions of possible structural isomers. Therefore, we apply a couple of semi-classical force-field global optimisation techniques that are presented in the following.

2.1. *Exploration of the Buckingham potential energy landscape*

Alumina (i.e. $Al_2O_3)_n$) and silicon carbide (i.e. $(SiC)_n$) candidate clusters structures are found with the Monte Carlo - Basin Hopping (MC-BH) global optimization technique (Wales *et al.* (1997)) with inter-atomic Buckingham pair potentials. The general form of the inter-atomic Buckingham pair potential reads:

$$U(r_{ij}) = \frac{q_i q_j}{r_{ij}} + A \exp(-\frac{r_{ij}}{B}) - \frac{C}{r_{ij}^6} \qquad (2.1)$$

where r_{ij} is the relative distance of two atoms, q_i and q_j the charges of atom i and j, respectively and A, B and C the Buckingham pair parameters. The first term represents the Coulomb law, the second term the short-range, steric repulsion term accounting for the Pauli principle, and the last term describes the van-der-Waals interaction. The steric repulsion term is motivated by the fact that atoms are not dot-like but occupy a certain volume in space.

The Buckingham pair potential parameters for Al-O systems are widely studied and the values are taken from Bush *et al.* (1994). In the case of silicon carbide, parameter sets for the Si-C system are lacking in the literature for several reasons. As an integral part the electrostatic Coulomb potential appears in Equation 2.1. It describes the repulsion and attraction of charged particles, in this case of Al and O, and Si and C. As lightest Group IV elements in the periodic table, Si and C form strong covalent bonds. However, the Buckingham potential is more suitable for materials with an ionic character and as for example metal oxides. Nonetheless, Watkins *et al.* (2009) have shown the similarity of zincblende ZnO (a cubic crystal type with face-centred lattice points), and β-SiC, despite the first is generally regarded as ionic II-VI system and the latter as covalent IV-IV system. Moreover, they found that the Buckingham parameters for ZnO also describe SiC clusters fairly well. Therefore, we performed MC-BH optimisations with a simplified version of the parameter set for ZnO given by Whitmore *et al.* (2002).

The ZnO forcefield we employ has been shown to be able to stabilize a wide range of different cluster isomers (Al-Sunaidi *et al.* (2008))) and bulk polymorphs (Demiroglu *et al.* (2014)) which exhibit alternating cation-anion ordering.. However, to reduce the probability to miss stable cluster isomers in our searches, we also ran some test calculations for several sizes with a forcefield parameterized for ZnS (Wright & Jackson (1995)) which potentially provides an additional source of cluster isomers not easily found with

the ZnO forcefield. However, the few structures that we found exclusively with the ZnS parameters had high energies (when converted to SiC clusters) and did not compete with the ZnO cluster analogues. Although the use of force fields is an approximation, their use enables us to perform tractable thorough searches. With our mixed-forcefield approach we hope to have minimized the probability to miss a stable SiC isomer.

2.2. *Tersoff potential simulated annealing*

Albeit the Buckingham pair potential including the Coulomb terms describes the force-field of ionic materials like metal oxides fairly well, it may fail to describe stable cluster configurations that are characterised by rather covalent than ionic bonds.

A simple two-body interaction is thus not sufficient to properly describe the Si-C system. In addition, a three-body potential is needed to describe the covalent character of bond bending and stretching (Stillinger & Weber (1985), Vishishta *et al.* (2007)). In order to properly describe internal interactions of the most stable SiC clusters, empirical bond-order potentials are favourable, in particular for small clusters (Erhart & Albe (2005)). This class of inter-atomic potentials include the Tersoff- type (Tersoff (1989)), the Brenner (Brenner (1990)), or, ReaxFF (Van Duin *et al.* (2001)), which take into account the bonding environment, namely bond lengths, bond angles and the number of bonds. As a consequence of geometry, the bonding angle in a tetrahedrally coordinated system like SiC is $\Theta = \arccos(-1/3) = 109.47°$. The general form of a bond-order potential reads:

$$V(r_{ij}) = f_c(r_{ij}) \left[V_{rep}(r_{ij}) + b_{ij} V_{att}(r_{ij}) \right] \tag{2.2}$$

where $V_{rep}(r_{ij}) = A_{ij} \exp\left(-\lambda_{ij} r_{ij}\right)$ is the repulsive part of the bond-order potential and $V_{att}(r_{ij}) = B_{ij} \exp\left(-\mu_{ij} r_{ij}\right)$ the attractive effective potential. b_{ij} modifies the strength of the bond, depending on the environmental parameter (the bonding angles Θ) as reported in Tersoff (1989). In the Tersoff parametrisation of inter-atomic Si-C molecular system, which is chosen in our approach, the potential is modified by a taper function f_c. f_c is 1 for inter-atomic distances r_{ij} smaller or equal of typical bonding distances and falls quickly to 0 for distances larger than S and thus restricts the interaction to the first neighbouring atoms within a distance S.

$$f_c(r_{ij}) = \begin{cases} 1, & r_{ij} < R \\ 0.5 + 0.5\cos(\frac{\pi(r_{ij}-R)}{S-R}), & R < r_{ij} < S \\ 0, & r_{ij} > S \end{cases} . \tag{2.3}$$

We use the programme GULP (General Utility Lattice Programme, Gale (1997)) which is taylored for the semi-classic parametrisation by Tersoff (1989).
Some SiC cluster structures have been reported in the literature (Pradhan & Ray (2004), Hou & Bin (2008), Duan *et al.* (2013). We tested their stability against (small) distortions in molecular dynamics runs with GULP. Furthermore, we applied the Tersoff potential to these structures. In the majority of the cases, this potential suffices to stabilise the structures. In some cases, however, the Tersoff potential fails to stabilize the clusters, and hand-constructed structures were taken instead for the subsequent computation. In some of these failure cases new, unreported clusters appeared.

2.3. *Quantum-mechanical refinement*

Once pre-optimised, the clusters are refined using quantum-mechanical DFT (Density Functional Theory) calculations to obtain structure-specific infrared spectra (i.e. vi-brational frequencies) rotational constants, and zero-point-energies. By comparing the

obtained infrared spectra with observational data, the specific isomers present in circumstellar envelopes can be identified. The $(Al_2O_3)_n$ and $(SiC)_n$ cluster structures, so far reported in the literature, rely on various theoretical quantum chemistry methods. They include DFT methods using generalized gradient approximation (GGA), local density approximation (LDA), hybrid functionals (e.g B3LYP, PBE0, M11), respectively, and post-Hartree Fock methods using Møller-Plesset (MP2, MBPT) and coupled-cluster (LCCD, CCSD) techniques.

For DFT methods the computational cost scales with the system size as between the order $\mathcal{O}(N^3)$ and $\mathcal{O}(N^4)$, where N is the number of electrons in the cluster. This means that they can be readily applied to systems containing 10s of atoms. However, many DFT methods can suffer from artificial electron self-interaction that results in overly strong electron delocalisation and too low potential energies. In contrast, Post-HartreeFock methods do not suffer from these effects. However, the computational cost of these latter methods is very high and scales with the system size as $\mathcal{O}(N^5)$-$\mathcal{O}(N^7)$. They are thus prohibitive for systems of more than approximately 10 atoms. Functionals such as B3LYP, M11 or PBE0 attempt to compensate for the above mentioned shortcomings of typical GGA/LDA functionals. The recent extensive benchmark study by Byrd et al. (2016) confirms that the M11 functional is able to correctly identify all investigated $(SiC)_n$ ground states. Although B3LYP Becke (1993) was found to be less accurate than M11 for SiC clusters, we also include data calculated with this widely used functional for comparison. We conclude that, for our purposes and for SiC, the M11 functional method is the best compromise between a reasonable computational cost and the required accuracy.

Owing to its high computational costs, DFT calculations are performed on supercomputers using the well-established and parallelised code *Gaussian 09*. These calculations approximate the wave functions and the energy of a quantum many-body system in a stationary state. *Gaussian 09* optimises cluster structures at a pressure of 0 bar and temperature of 0 K. We account for circumstellar conditions (temperatures and pressures) by applying thermodynamic potential functions (enthalpy, entropy, Gibbs energy) that are evaluated with the help of partition functions. These functions and their derivatives are calculated from the electronic energies, moments of inertia and vibrational frequencies within the rigid-rotor harmonic oscillator approximation (McQuarrie & Simon (1999), Goumans & Bromley (2012)).

As a consequence, the relative energy spacings of the individual clusters shift and may cross. This implies that the initial lowest energy isomer may not be the most favourable structure in circumstellar conditions and a different cluster structure is preferred. It is thus necessary to study a range of the energetically lowest-lying structures for each cluster size. The use of partition functions relies on the validity of thermodynamic equilibrium. We note, however, that AGB atmospheres may depart from equilibrium as they are periodically crossed by pulsational shock waves. The resulting Gibbs Free energies thus have limited validity. Nonetheless, they provide a good approximation for the individual cluster stability in circumstellar conditions.

3. Results

3.1. *Alumina clusters*

In Figure 2, the $(Al_2O_3)_n$, $n = 1-10$ isomers with the lowest potential energies are shown. For n=8, 9, and 10 we found new global minima candidates that are in part reported in Gobrecht et al. (2018). The minima isomers exhibit a variety of different structural features, and no attribute, apart from alternating Al-O bonds, is common to all these
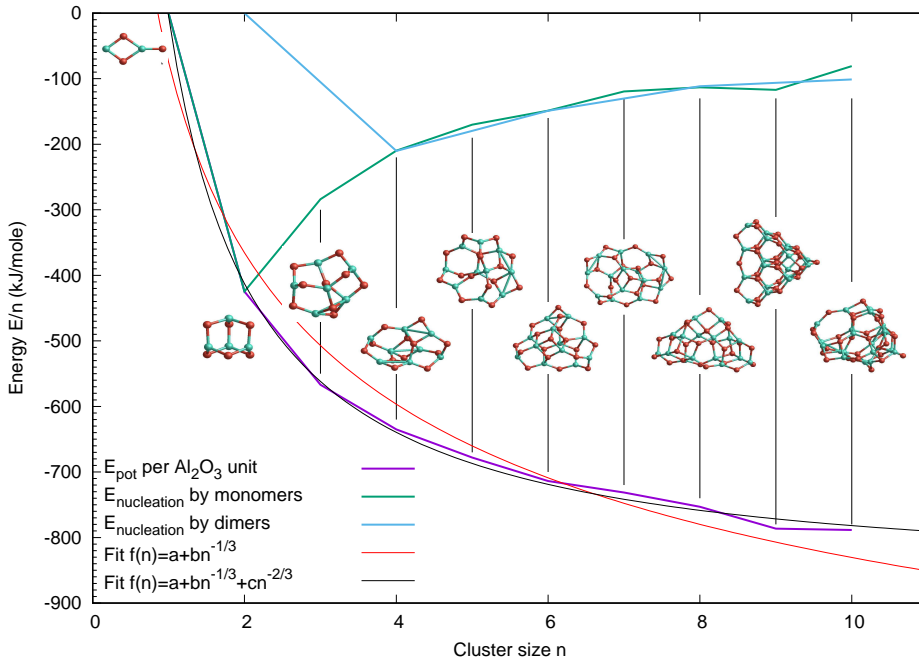
Figure 2. The global minima $(Al_2O_3)_n$, $n = 1-10$, candidate isomers and their potential energies (in purple), nucleation energies (by monomers in green, by dimers in blue), and related first (in red) and second order (in black) fits. Oxygen atoms are in red, Aluminum atoms in green.

minima clusters. For this reason, a fit function $f(n)=a+bn^{-\frac{1}{3}}$ to the normalised potential energy oversimplifies the size dependence in energy. Including a second-order term $cn^{-\frac{2}{3}}$ in the fit function describes the size-dependence of the potential energy $E(n)$ better, though not perfectly. Moreover, we show that the nucleation energies by monomer addition, $E_{nuc}(n)=E(n)-E(n-1)- E(1)$, as well as by dimer addition $E_{nuc}(n)=E(n)-E(n-2)-E(2)$, have negative energies and thus a nucleation is viable. There are no energetic barriers in homogeneous nucleation scenarios, but the initial steps (dimerisation and dimer coalescense) are expected to be the fastest steps, as they are the most exothermic processes. The vibrational IR spectra is shown in Figure 3. The most intense vibrations of the clusters are located in a wavelength range between 10 and 12 μm. Around 13 μm, where is the alumina dust feature is located, the overall intensity is rather low. Along with other characteristics (bond length, coordination), we conclude that, at the size of the decamers (n=10), the bulk limit for alumina clusters is not yet reached.

3.2. *Silicon carbide clusters*

The silicon carbide clusters have been extensively discussed in Gobrecht *et al.* (2017). The most stable isomers are dominated by two structural families: void cage geometries with strict cation-anion ordering ("bucky"-like) and segregated clusters exhibiting chains and rings of carbon. The binding energy ΔE_b of the lowest-energy Si_nC_n clusters as well as the HOMO (Highest Occupied Molecular Orbital)−LUMO (Lowest Unccupied Molecular Orbital) energy gap ΔE_{MO} are presented in Figure 4.

The binding energies ΔE_b of the global minima clusters generally increase with cluster size. However, some cluster sizes ($n =9,12$) appear to be more stable than the next larger cluster of size $n + 1 =10,13$. In the HOMO-LUMO energies, no clear trend with
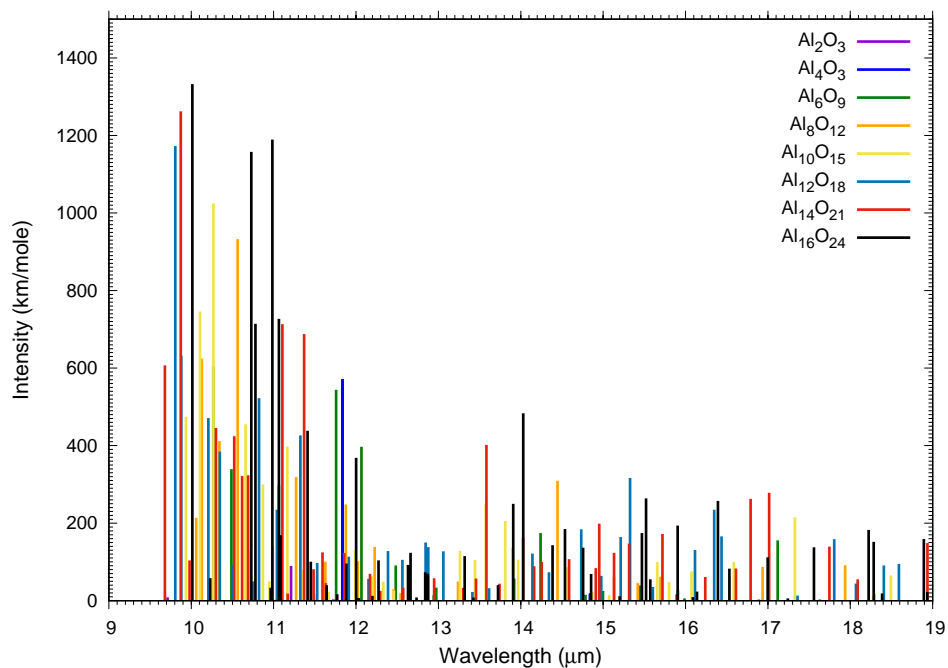
Figure 3. The vibrational IR spectra of the global minima $(Al_2O_3)_n$, $n =1-8$, clusters as a function of wavelength .

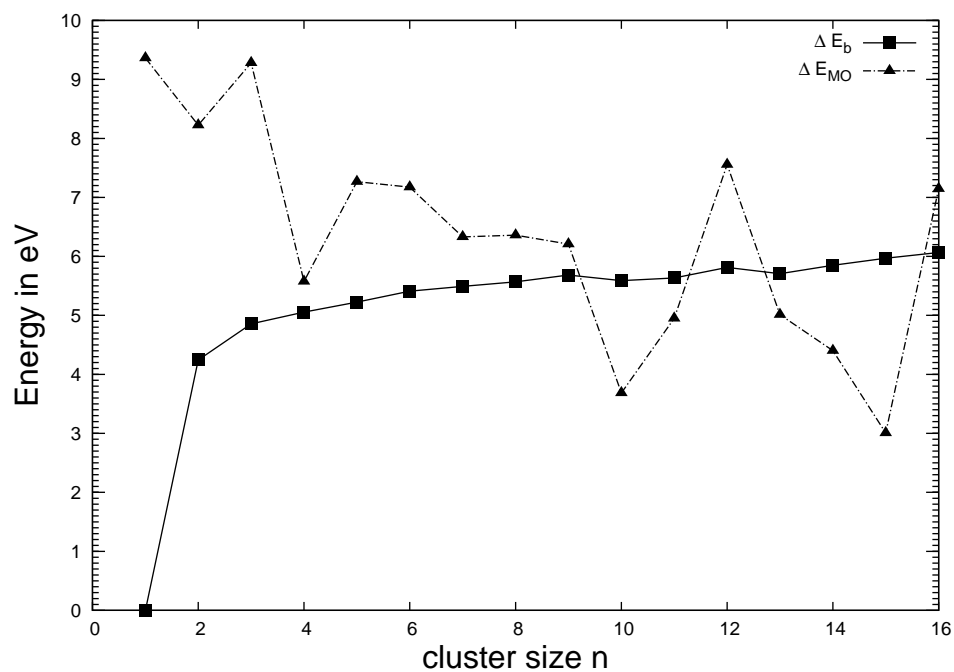**Figure 4.** The relative binding energy ΔE_b (filled squares and solid line) of the global minima Si_nC_n clusters (normalised to cluster size n) and the HOMO-LUMO energy gap ΔE_{MO} (triangles and dashed line) of the ground state Si_nC_n clusters

cluster size n is observed. The "bucky"-like clusters show strong vibrational IR signatures, compared with their segregated counterparts. This fact is illustrated in Figure 5, where the structure-specific opacity, derived from the IR intensity, is displayed as a function of wavelength.
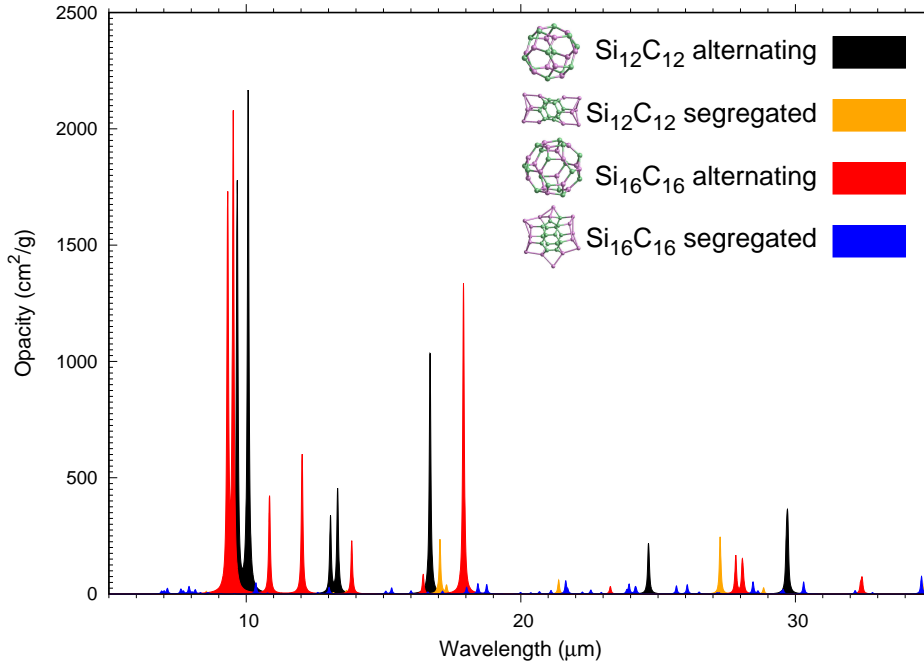

Figure 5. The energetically most favourable $(SiC)_n$ clusters of each structural family (alternating and segregated) and their relative potential energies in kJ/mole Silicon atoms are in pink, carbon atoms in green .

References

Al-Sunaidi, A. A., Sokol, A. A., Catlow C. R. A., Woodley, S. M. 2008, *JPCC*, 112, 18860

Agúndez, M., Cernicharo, J., Guélin, M., 2010, *ApJ*, 724, 133

Becke, A. D. 1993, *JCP*, 98, 1372

Brenner, D. W. 1990, *Phys. Rev. B*, 42, 9458

Bromley, S. T., Gómez-Martín, J. C., Plane, J. M. C. 2016, *PCCP*, 18, 26913

Bush, T. S., Gale, J. D., Catlow, C. R. A., Battle, P. D. 1994, *JMC*, 4, 831

Byrd, J. N. and Lutz, J. J., Jin, Y. Ranasinghe, D. S., Montgomery, J. A., Perera, A., Duan, X. F., Burggraf, L. W., Sanders, B. A., Bartlett, R.J. 2016, *JCP*, 145, 24312

Chen, M., Felmy, A. R., Dixon, D. A. 2014, *JPCA*, 118, 3136

Decin, L., De Beck, E., Brnken, S., Mller, H. S. P., Menten, K. M., Kim, H., Willacy, K., de Koter, A., Wyrowski, F. 2010, *A&A*, 516, 69

Decin, L., Justtanont, K., De Beck, E., Lombaert, R., de Koter, A., Waters, L. B. F. M., Marston, A. P., Teyssier, D., Schier, F. L., Bujarrabal, V., Alcolea, J., Cernicharo, J., Dominik, C., Melnick, G., Menten, K., Neufeld, D. A., Olofsson, H., Planesas, P., Schmidt, M., Szczerba, R., de Graauw, T., Helmich, F., Roelfsema, P., Dieleman, P., Morris, P., Gallego, J. D., Dez-Gonzlez, M. C., Caux, E. 2010, *A&A*, 521, 4

Decin, L., Richards, A. M. S., Waters, L. B. F. M., Danilovich, T., Gobrecht, D., Khouri, T., Homan, W., Bakker, J. M., Van de Sande, M., Nuth, J. A., De Beck, E. 2017, *A&A*, 608, 55

Demiroglu, I., Tosoni, S. and Illas, F., Bromley, S. T. 2014, *Nanoscale* 6, 1181

Duan, X. F., Burggraf, L. W., Huang, L. 2013, *Molecules*, 18, 8591

Erhart, P., Albe, K. 2005, *Phys. Rev. B*, 71, 35211

Gale, J. D. 1997, *JCS, Faraday Trans.*, 93, 629

Gobrecht, D., Cherchneff, I., Sarangi, A., Plane, J. M. C., Bromley, S. T. 2016, *A&A*, 585, 15

Gobrecht, D., Cristallo, S., Piersanti, L., Bromley, S. T. *ApJ*, 840, 117

Gobrecht, D., Decin, L., Cristallo, S., Bromley, S. T. *CPLett*, 711, 138

Goumans, T. P. M., Bromley, S. T. 2012, *MNRAS*, 420, 3344

Habing, H. J., Olofsson, H. 2004, *A&A library*

Henning, Th. 2010, *Lecture Notes in Physics*, 815

Hoefner, S., GautschyLoidl, R., Aringer, B., Jørgensen, U.G. 2003, *A&A*, 399, 589

Hou, J., Song, B. 2008, *JCP*, 128,154304

Johansson, L. E. B., Andersson, C., Ellder, J., Friberg, P., Hjalmarson, A., Hoglund, B., Irvine, W. M., Olofsson, H., Rydbeck, G. 1984, *A&A*, 130, 227

Justtanont, K., Feuchtgruber, H., de Jong, T., Cami, J., Waters, L. B. F. M., Yamamura, I., Onaka, T. 1998, *A&A*, 330, 17

Karovicova, I., Wittkowski, M., Ohnaka, K., Boboltz, D. A., Fossat, E., Scholz, M. 2013, *A&A*, 560, 75

Koehler, T. M., Gail, H.-P., Sedlmayr, E. 1997, *A&A*, 320, 553

Lamiel-Garcia, O., Ko, K. C., Lee, J. Y., Bromley, S. T., Illas, F. *JCTC*, 13, 1785

Li, R., Cheng, L. 2012, *CTP*, 996, 125

Lindqvist, M., Nyman, L.-A., Olofsson, H., Winnberg, A. 1988, *A&A*, 205, 15

McQuarrie, D. A., Simon, J. D. 1999, *University Science Books*

Neufeld, D. A., Gonzlez-Alfonso, E., Melnick, G. J., Szczerba, R., Schmidt, M., Decin, L, de Koter, A., Schier, F., Cernicharo, J. 2011, *APJL*, 727, 28

Peverati, R., Truhlar, D. G. 2012, *JPCL* 3, 117

Posch, T., Kerschbaum, F., Mutschke, H., Fabian, D., Dorschner, J., Hron, J. 1999, *A&A*, 352, 609

, Pradhan, P., Ray, A. K. 2004, *ArXiv Physics e-prints*, 0408016

Sloan, G. C., Kraemer, K. E., Goebel, J. H., Price, S. D. 2003, *ApJ*, 594, 483

Stillinger, F. H. & Weber, T. A. 1985, 31, 5262

Stroud, R. M., Nittler, L. R., Alexander, C. M. O'D. 2004, *Science* 305, 1455

Tersoff, J. 1989, *Phys. Rev. B*, 39, 5566

Treffers, R., Cohen, M. 1974, *ApJ* 188, 545

Van de Sande, M., Sundqvist, J. O., Millar, T. J., Keller, D., Homan, W., de Koter, A., Decin, L., De Ceuster, F. 2018, *A&A*, 616, 106

Van Duin, A. C. T., Dasgupta, F., Lorant, F. Goddard, W. A. 2001, *JPCA*, 105, 9396

Vashishta, P., Kalia, R. K., Nakano, A., Rino, J. P. 2007, *JAP* 10, 101

Wales, D. J., Doye, J. P. K. 1997, *JPCA*, 101, 5111

Watkins, M. B., Shevlin, S. A., Sokol, A. A., Slater, B., Catlow, C. R. A., Woodley, S. M. *PCCP*, 11, 3186

Wetzel, S., Klevenz, M., Gail, H.-P., Pucci, A., Trieloff, M. *A&A*, 553, 92

Whitmore, L., Sokol, A. A., Catlow, C. R. A. 2002, *Surface science*, 498, 135

Wright, K., Jackson, R. A. 1995, *JMC*, 5, 2037

Woitke, P. 2006, *A&A*, 460, 9

Discussion

DeBeck: Where in the spectrum do you expect the vibrational modes of the alumina clusters?

Gobrecht: The most intense vibration bands are located in a wavelength range between $\sim 10-11\mu$m, but I also find less intense IR modes at $\sim 13\mu$m (where the observed Al-O stretching modes are found).